here we focused on chromosomal segregation from the 1-cell to the 8-cell stage, which is critical for postimplantation development. Monomeric red fluorescent protein coupled with histone H2B (mRFP–H2B) and EGFP-tagged α-tubulin were expressed in embryos by mRNA injection immediately after SCNT or intracytoplasmic sperm injection (ICSI) and chromosomal segregation was monitored. Some embryos at these stages showed abnormal chromosomal behavior in mitotic blastomeres. Parts of the chromosomes were misaligned with the metaphase plate and lagging chromosomes were found at anaphase (Figure 1A). Consequently, ectopic micronuclei appeared as a result of ACS (Figure 1B-D). The incidence of ACS in cloned embryos produced with CB treatment was significantly higher than in ICSI-generated control embryos at the first, second and third cell division. However, when using LatA instead of CB, the incidence of ACS decreased significantly at the 2-cell stage and became similar to control embryos at the 4-cell and 8-cell stages (Figure 1E).

Epigenetic abnormalities in cloned embryos produced with CB or LatA

Our next question was whether the increased success rate of cloned mice produced by LatA treatment arose from modifications of epigenetic abnormalities. To investigate this, CB- or LatA-treated cloned embryos and ICSI-generated embryos were fixed at the pronuclear stage and immunostained with antibodies to acetylated histone H3 at lysines 9 or 14 (acH3K9 or acH3K14, respectively), to H3K9me2, to dimethylated histone H3 at lysine 14 (H3K14me2) and to H2B. As shown in Figure 2, the acetylation or methylation levels were not different between CB- and LatA-treated cloned embryos, but were abnormally high or low, respectively, compared with control embryos.

Epigenetic abnormalities in cloned placentae produced with CB or LatA treatments

It is well known that most cloned animals possess abnormal placentae arising from epigenetic errors [36-38]. Placentae derived from cloned or ICSI-generated control embryos were collected at embryonic day (E)19.5 and their weights and histology were compared. Abnormally heavy placentae and the abnormal distortion of the boundary between spongiotrophoblast and labyrinth layers were not corrected with LatA treatment (Figure 3).

Effect of BIX-01294 on cloned preimplantation embryos

H3K9me2 plays an important role in gene silencing but so far no cloning method has been able to correct abnormally high H3K9me levels in cloned embryos. We tried to control the H3K9me2 status in cloned embryos by using BIX, a specific inhibitor of the G9a histone methyltransferase. First, we examined the maximum concentration of BIX that did not decrease the blastocyst formation rate in control embryos and decided to use 3 nM, which led to the highest blastocyst formation rate. (Figure 4A). Then we examined the effect of this treatment on cloned embryos in terms of G9a target gene expression and H3K9me2 level. Real-time RT–PCR was performed at the blastocyst stage using ICSI-generated, control cloned embryos and BIX-treated cloned embryos. As shown in Figure 4B, *Magea2* gene expression was significantly upregulated by BIX treatment ($P < 0.05$). This result is consistent with the report that *Magea2* expression in ES cells is controlled by G9a through H3K9me2 at the promoter site [26]. When 1-cell stage cloned embryos were examined by immunostaining, BIX treatment decreased the H3K9me2, HP1α and acH3K9 levels significantly (Figure 4C–F; $P < 0.05$).

Effects of BIX on full-term development of cloned embryos

Finally, we examined whether correcting the epigenetic abnormalities at H3K9me2 in cloned embryos could lead to full-term development. Although BIX treatment reduced the level of H3K9me2 in cloned preimplantation embryos, the birth rate of cloned mice following BIX treatment was 7.8% (8/102), almost the same as untreated controls (7.3%, 9/123; Table 1). Thus, alleviating this particular epigenetic aberration in cloned embryos did not improve development to term.

Discussion

Previously, we reported that LatA treatment corrected aberrant F-actin localization in cloned embryos and increased the birth rate of cloned mice [20]. However, the association between inhibition of actin polymerization at the 1-cell stage and full-term development was not clear. F-actin in the nucleus has an important role in chromosome transport [24] and cloned embryos exhibiting ACS before the 8-cell stage cannot develop to full term [25]. We confirmed here that the occurrence of ACS was significantly higher than controls in CB-treated cloned embryos at the 2-cell stage, but this decreased significantly to the same level as ICSI-generated embryos when using LatA instead of CB. Thus, LatA appears to improve the birth rate associated with ACS in cloned embryos by gently inhibiting actin polymerization; importantly, this event was not linked directly to epigenetic alterations. When specific histone modifications associated with either active (acH3K9 and H3K4me2) or repressed (H3K9me2) chromatin, and with aberrant spindles in oocytes (acH3K14) [27,28] were examined, these were not improved by using LatA instead of CB.

Next, we focused on the H3K9me2 abnormality in cloned embryos because its level decreases quickly in normally fertilized embryos to allow the proper expression of several genes but persists in cloned embryos [6,12,13,39-42]. This methylated histone region serves as a binding platform for HP1 [14,15,43]; correspondingly, HP1 expression was significantly higher in cloned embryos than in zygotes fertilized in vitro [44]. In addition, H3K9-related genes, such as *Magea* and *Xlr*, also failed to be expressed in cloned embryos even when the expression of *Xist* was controlled [10].

In this study, we used BIX as a specific inhibitor of G9a [27]. The H3K9me2 level at the *Magea2* promoter region was decreased by BIX treatment [26]. Consistent with this result, when we treated cloned embryos with BIX, H3K9me2 and HP1α levels were significantly decreased and *Magea2* gene

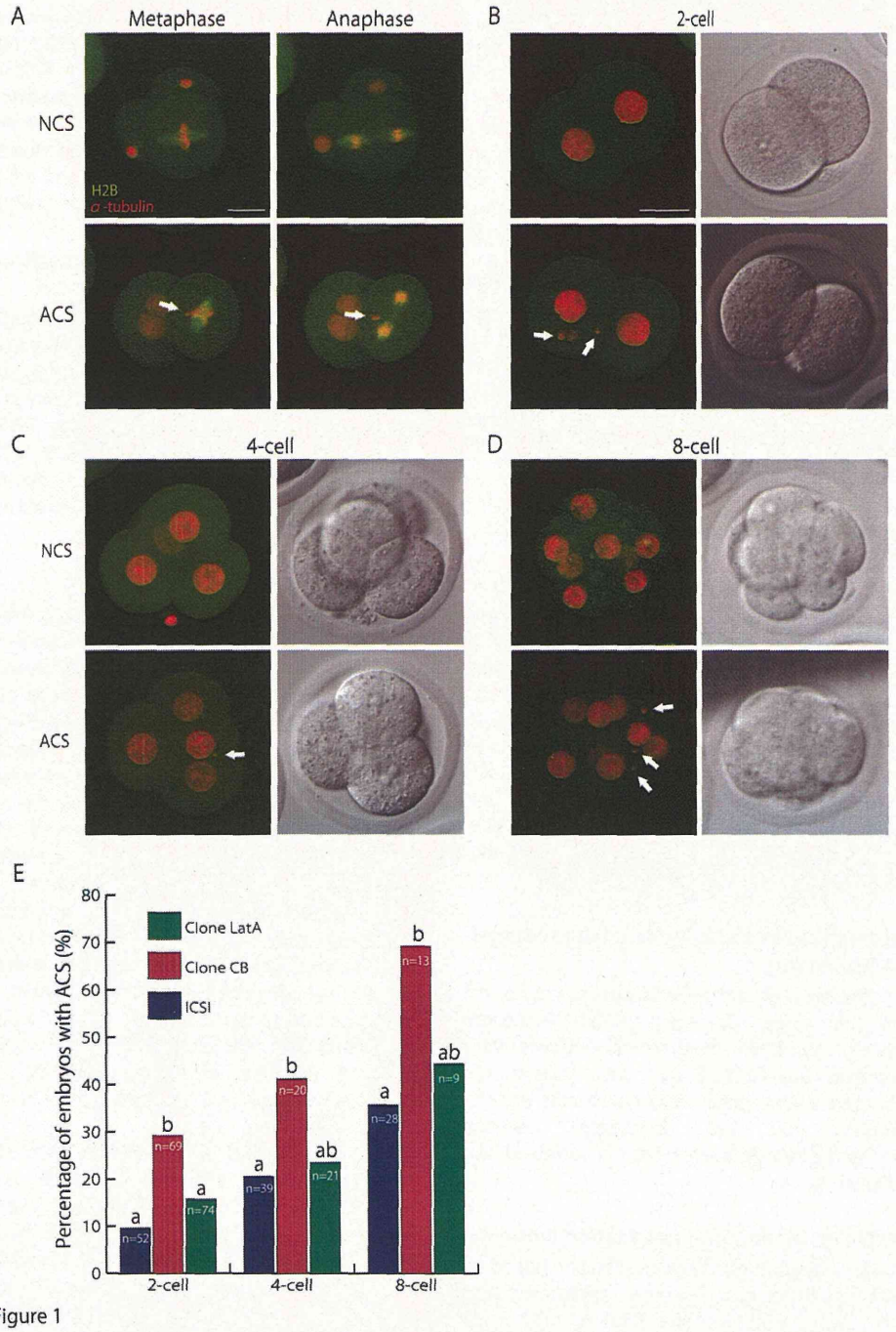

Figure 1

Figure 1. Chromosome segregation in early embryonic development. (A) Chromosomes were misaligned at metaphase and lagging chromosomes were found at anaphase in embryos ACS was occured. (B-D) Merged and bright field images of embryos with normal chromosomal segregation (NCS) and abnormal chromosomal segregation (ACS). As an example, time-lapse images of chromosome segregation at the first, second and third mitosis are shown at the 2-cell, 4-cell and 8-cell stages, respectively. Arrows indicate chromosomal fragments appearing during the division. Green, EGFP-α-tubulin; red, mRFP–H2B. Bar = 30 μm. (E) The percentages of embryos with ACS at the 2-cell, 4-cell and 8-cell stages in ICSI-generated and cloned embryos. Values with different superscripts in the same category differ significantly between ICSI-generated, CB- and LatA-treated cloned embryos.

doi: 10.1371/journal.pone.0078380.g001

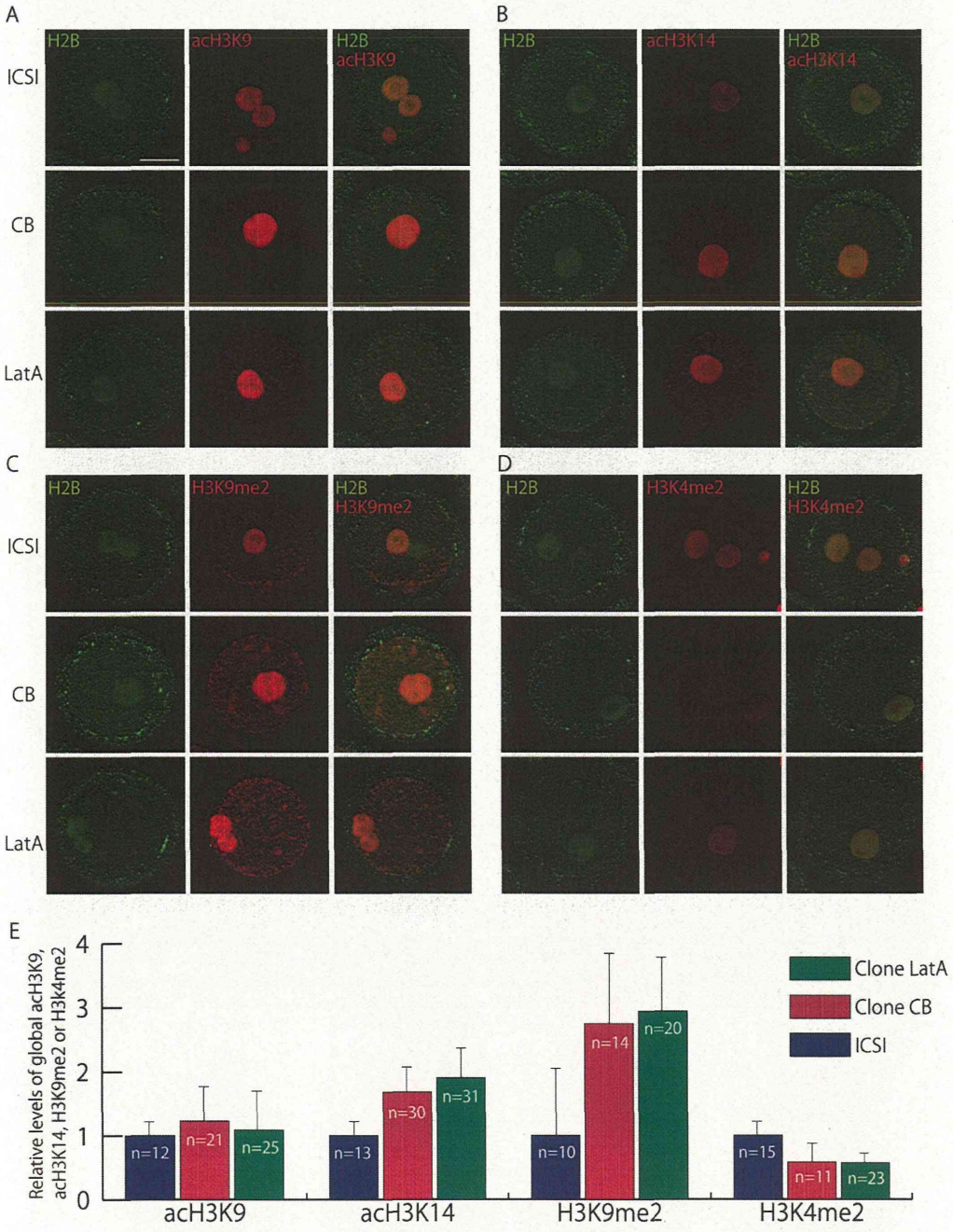

Figure 2

Figure 2. Histone modifications in 1-cell stage embryos. (A-D) acH3K9, acH3K14, H3K9me2 or H3K4me2 levels in ICSI-generated and CB- or LatA-treated cloned embryos. Bar = 30 μm. (E) The intensities of immunofluorescence for acH3K9, acH3K14, H3K9me2 and H3K4me2 relative to that of H2B. They are compared with the intensities in ICSI-generated control embryos. The acetylation or methylation levels of these regions were not different between LatA- and CB-treated cloned embryos.

doi: 10.1371/journal.pone.0078380.g002

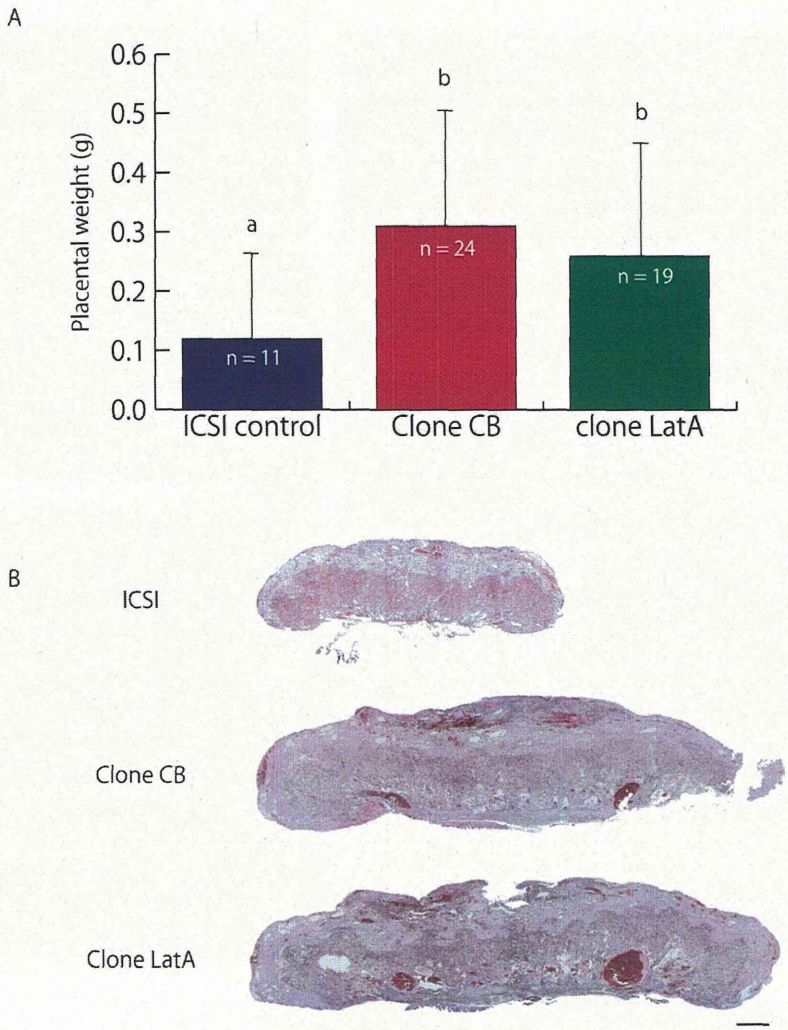

Figure 3

Figure 3. Abnormalities in placentae derived from cloned embryos. (A) Placental weights from ICSI-derived control embryos and CB- or LatA-treated cloned embryos. Error bars indicate SD. Asterisks indicate significant difference at $p < 0.05$. (B) Hematoxylin and eosin staining of placentae derived from ICSI-derived control and CB- or LatA-treated cloned embryos. Abnormal distortion of the boundary between the spongiotrophoblast and labyrinth layers was observed in placentas derived from both CB- and LatA-treated cloned embryos. Bar = 500 μm.

doi: 10.1371/journal.pone.0078380.g003

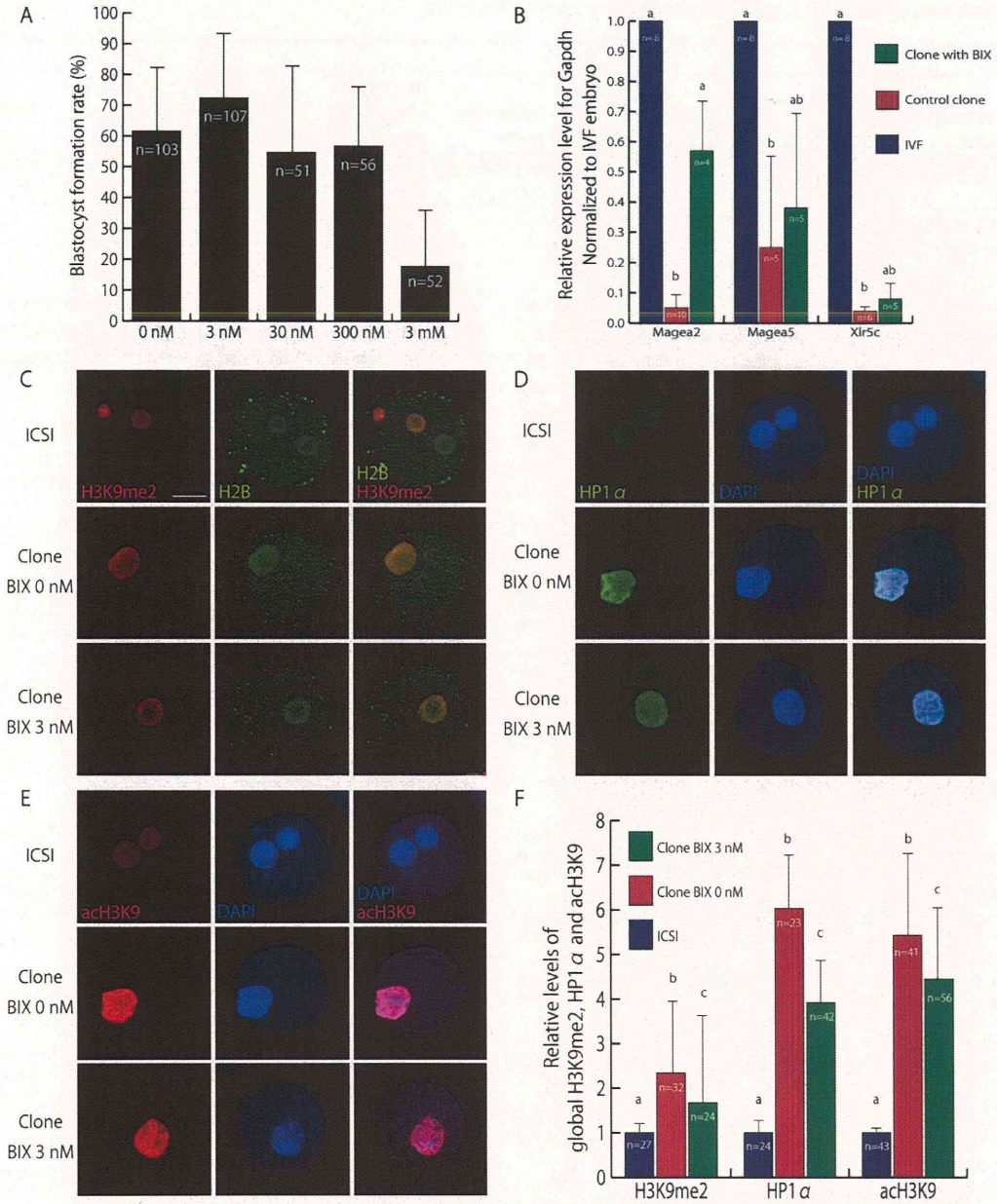

Figure 4

Figure 4. The effect of BIX on cloned embryos. (A) Blastocyst formation rate of cloned embryos treated with various concentrations of BIX. (B) Relative expression level of *Magea* and *Xlr* family genes in a blastocyst. The level of mRNA was normalized to the *Gapdh* expression level in the same sample. These genes were strongly repressed in control cloned blastocysts, but the reduced *Magea2* expression was increased by treatment with BIX. (C–F) Fluorescence level of H3K9me2, HP1α and acH3K9 normalized to the DAPI or histone H2B level of the same sample. Bar = 30 μm. BIX treatment was effective in decreasing H3K9me2, HP1α and acH3K9 levels.

doi: 10.1371/journal.pone.0078380.g004

Table 1. The effect of BIX on full term development of cloned embryos.

Treatment	No. reconstructed oocytes	No. survived after activation	No. PN formed	No. 2-cell embryos (%/PN)	No. morulae (%/PN)	No. embryos transferred (recipients)	No. live offspring (%/ET)	Mean body weight (g)	Mean placental weight (g)
Control	239	178	160	146 (91.3)	123 (76.9)	123 (13)	9 (7.3)	1.80 ± 0.24	0.30 ± 0.09
BIX 3 nM	194	152	140	125 (89.3)	102 (72.9)	102 (8)	8 (7.8)	2.12 ± 0.43	0.33 ± 0.04

PN, pronuclei; ET, embryo transfer

doi: 10.1371/journal.pone.0078380.t001

expression was improved, while the expression levels of *Magea5* and *Xlr5c* were not increased significantly. However, the birth rate of cloned mice was not increased at all. Surprisingly, the acH3K9 level decreased, so several other H3K9me-related genes might remain silenced in BIX-treated cloned embryos and thereby lead to embryo death. Because Xist knockout or knockdown did not change the expression patterns of *Magea* and *Xlr* family genes in cloned embryos [6,10], H3K9me2 might be a reprogramming-resistant region of the SCNT nucleus, and other approaches targeting these sites might be needed for proper genomic reprogramming.

In conclusion, while BIX treatment did not increase the birth rate of cloned mice even though some epigenetic errors were corrected to some extent, LatA treatment promoted normal chromosome segregation in the context of proper F-actin formation and improved the full-term development of cloned embryos with epigenetic abnormalities remained. Thus, non-epigenetic factors, such as F-actin formation and chromosome segregation in early stage of preimplantation embryos, also play an important role in determining the success rate of mouse cloning.

Acknowledgements

We are grateful to the Laboratory for Animal Resources and Genetic Engineering for housing the mice.

Author Contributions

Conceived and designed the experiments: YT KY TW. Performed the experiments: YT MT FI. Analyzed the data: YT. Contributed reagents/materials/analysis tools: YT SW CL. Wrote the manuscript: YT TW. Supported doing experiments and writing the manuscript: ES KT.

References

1. Jullien J, Pasque V, Halley-Stott RP, Miyamoto K, Gurdon JB (2011) Mechanisms of nuclear reprogramming by eggs and oocytes: a deterministic process? Nat Rev Mol Cell Biol 12: 453-459. doi:10.1038/nrg3034. PubMed: 21697902.
2. Kim K, Doi A, Wen B, Ng K, Zhao R et al. (2010) Epigenetic memory in induced pluripotent stem cells. Nature 467: 285-290. doi:10.1038/nature09342. PubMed: 20644535.
3. Wilmut I, Schnieke AE, McWhir J, Kind AJ, Campbell KH (1997) Viable offspring derived from fetal and adult mammalian cells. Nature 385: 810-813. doi:10.1038/385810a0. PubMed: 9039911.
4. Wakayama T, Perry AC, Zuccotti M, Johnson KR, Yanagimachi R (1998) Full-term development of mice from enucleated oocytes injected with cumulus cell nuclei. Nature 394: 369-374. doi:10.1038/28615. PubMed: 9690471.
5. Thuan NV, Kishigami S, Wakayama T (2010) How to improve the success rate of mouse cloning technology. J Reprod Dev 56: 20-30. doi:10.1262/jrd.09-221A. PubMed: 20203432.
6. Inoue K, Kohda T, Sugimoto M, Sado T, Ogonuki N et al. (2010) Impeding Xist Expression from the Active X Chromosome Improves Mouse Somatic Cell Nuclear Transfer. Science, 330: 496–9. PubMed: 20847234.
7. Ono T, Li C, Mizutani E, Terashita Y, Yamagata K et al. (2010) Inhibition of class IIb histone deacetylase significantly improves cloning efficiency in mice. Biol Reprod 83: 929-937. doi:10.1095/biolreprod.110.085282. PubMed: 20686182.
8. Wakayama S, Cibelli JB, Wakayama T (2003) Effect of timing of the removal of oocyte chromosomes before or after injection of somatic nucleus on development of NT embryos. Cloning Stem Cells 5: 181-189. doi:10.1089/153623003769645848. PubMed: 14588136.
9. Ogura A, Inoue K, Wakayama T (2013) Recent advancements in cloning by somatic cell nuclear transfer. Philos Trans R Soc Lond B Biol Sci 368: 20110329. PubMed: 23166393.
10. Matoba S, Inoue K, Kohda T, Sugimoto M, Mizutani E et al. (2011) RNAi-mediated knockdown of Xist can rescue the impaired postimplantation development of cloned mouse embryos. Proc Natl Acad Sci U S A 108: 20621-20626. doi:10.1073/pnas.1112664108. PubMed: 22065773.
11. Kishigami S, Mizutani E, Ohta H, Hikichi T, Thuan NV et al. (2006) Significant improvement of mouse cloning technique by treatment with trichostatin A after somatic nuclear transfer. Biochem Biophys Res Commun 340: 183-189. doi:10.1016/j.bbrc.2005.11.164. PubMed: 16356478.
12. Wang F, Kou Z, Zhang Y, Gao S (2007) Dynamic reprogramming of histone acetylation and methylation in the first cell cycle of cloned mouse embryos. Biol Reprod 77: 1007-1016. doi:10.1095/biolreprod.107.063149. PubMed: 17823087.
13. Bui HT, Wakayama S, Kishigami S, Park KK, Kim JH et al. (2010) Effect of trichostatin A on chromatin remodeling, histone modifications, DNA replication, and transcriptional activity in cloned mouse embryos. Biol Reprod 83: 454-463. doi:10.1095/biolreprod.109.083337. PubMed: 20505166.
14. Bannister AJ, Zegerman P, Partridge JF, Miska EA, Thomas JO et al. (2001) Selective recognition of methylated lysine 9 on histone H3 by the HP1 chromo domain. Nature 410: 120-124. doi:10.1038/35065138. PubMed: 11242054.
15. Lachner M, O'Carroll D, Rea S, Mechtler K, Jenuwein T (2001) Methylation of histone H3 lysine 9 creates a binding site for HP1 proteins. Nature 410: 116-120. doi:10.1038/35065132. PubMed: 11242053.
16. Smothers JF, Henikoff S (2001) The hinge and chromo shadow domain impart distinct targeting of HP1-like proteins. Mol Cell Biol 21: 2555-2569. doi:10.1128/MCB.21.7.2555-2569.2001. PubMed: 11259603.
17. Yu Y, Ding C, Wang E, Chen X, Li X et al. (2007) Piezo-assisted nuclear transfer affects cloning efficiency and may cause apoptosis. Reproduction 133: 947-954. doi:10.1530/REP-06-0358. PubMed: 17616724.
18. Balbach ST, Jauch A, Böhm-Steuer B, Cavaleri FM, Han YM et al. (2007) Chromosome stability differs in cloned mouse embryos and derivative ES cells. Dev Biol 308: 309-321. doi:10.1016/j.ydbio.2007.05.034. PubMed: 17610862.

19. Balbach ST, Esteves TC, Houghton FD, Siatkowski M, Pfeiffer MJ et al. (2012) Nuclear reprogramming: kinetics of cell cycle and metabolic progression as determinants of success. PLOS ONE 7: e35322. doi: 10.1371/journal.pone.0035322. PubMed: 22530006.
20. Terashita Y, Wakayama S, Yamagata K, Li C, Sato E et al. (2012) Latrunculin a can improve the birth rate of cloned mice and simplify the nuclear transfer protocol by gently inhibiting actin polymerization. Biol Reprod 86: 180. doi:10.1095/biolreprod.111.098764. PubMed: 22492972.
21. Wakayama T, Yanagimachi R (2001) Effect of cytokinesis inhibitors, DMSO and the timing of oocyte activation on mouse cloning using cumulus cell nuclei. Reproduction 122: 49-60. doi:10.1530/rep.0.1220049. PubMed: 11425329.
22. Miyamoto K, Gurdon JB (2012) Transcriptional regulation and nuclear reprogramming: roles of nuclear actin and actin-binding proteins. Cell Mol Life Sci, 70: 3289–302. PubMed: 23275942.
23. Miyamoto K, Pasque V, Jullien J, Gurdon JB (2011) Nuclear actin polymerization is required for transcriptional reprogramming of Oct4 by oocytes. Genes Dev 25: 946-958. doi:10.1101/gad.615211. PubMed: 21536734.
24. Mori M, Monnier N, Daigle N, Bathe M, Ellenberg J et al. (2011) Intracellular transport by an anchored homogeneously contracting F-actin meshwork. Curr Biol 21: 606-611. doi:10.1016/j.cub.2011.03.002. PubMed: 21439825.
25. Mizutani E, Yamagata K, Ono T, Akagi S, Geshi M et al. (2012) Abnormal chromosome segregation at early cleavage is a major cause of the full-term developmental failure of mouse clones. Dev Biol 364: 56-65. doi:10.1016/j.ydbio.2012.01.001. PubMed: 22266425.
26. Kubicek S, O'Sullivan RJ, August EM, Hickey ER, Zhang Q et al. (2007) Reversal of H3K9me2 by a small-molecule inhibitor for the G9a histone methyltransferase. Mol Cell 25: 473-481. doi:10.1016/j.molcel.2007.01.017. PubMed: 17289593.
27. Tachibana M, Sugimoto K, Nozaki M, Ueda J, Ohta T et al. (2002) G9a histone methyltransferase plays a dominant role in euchromatic histone H3 lysine 9 methylation and is essential for early embryogenesis. Genes Dev 16: 1779-1791. doi:10.1101/gad.989402. PubMed: 12130538.
28. Rice JC, Briggs SD, Ueberheide B, Barber CM, Shabanowitz J et al. (2003) Histone methyltransferases direct different degrees of methylation to define distinct chromatin domains. Mol Cell 12: 1591-1598. doi:10.1016/S1097-2765(03)00479-9. PubMed: 14690610.
29. Chatot CL, Lewis JL, Torres I, Ziomek CA (1990) Development of 1-cell embryos from different strains of mice in CZB medium. Biol Reprod 42: 432-440. doi:10.1095/biolreprod42.3.432. PubMed: 2111184.
30. Kimura Y, Yanagimachi R (1995) Intracytoplasmic sperm injection in the mouse. Biol Reprod 52: 709-720. doi:10.1095/biolreprod52.4.709. PubMed: 7779992.
31. Nakagata N (1996) Use of cryopreservation techniques of embryos and spermatozoa for production of transgenic (Tg) mice and for maintenance of Tg mouse lines. Lab Anim Sci 46: 236-238. PubMed: 8723247.
32. Yamagata K, Suetsugu R, Wakayama T (2009) Assessment of chromosomal integrity using a novel live-cell imaging technique in mouse embryos produced by intracytoplasmic sperm injection. Hum Reprod 24: 2490-2499. doi:10.1093/humrep/dep236. PubMed: 19574276.
33. Kishigami S, Wakayama T (2007) Efficient strontium-induced activation of mouse oocytes in standard culture media by chelating calcium. J Reprod Dev 53: 1207-1215. doi:10.1262/jrd.19067. PubMed: 17938555.
34. Yamagata K, Suetsugu R, Wakayama T (2009) Long-term, six-dimensional live-cell imaging for the mouse preimplantation embryo that does not affect full-term development. J Reprod Dev 55: 343-350. doi:10.1262/jrd.20166. PubMed: 19305125.
35. Yamagata K (2010) DNA methylation profiling using live-cell imaging. Methods 52: 259-266. doi:10.1016/j.ymeth.2010.04.008. PubMed: 20412856.
36. Tanaka S, Oda M, Toyoshima Y, Wakayama T, Tanaka M et al. (2001) Placentomegaly in cloned mouse concepti caused by expansion of the spongiotrophoblast layer. Biol Reprod 65: 1813-1821. doi:10.1095/biolreprod65.6.1813. PubMed: 11717146.
37. Ohgane J, Wakayama T, Kogo Y, Senda S, Hattori N et al. (2001) DNA methylation variation in cloned mice. Genesis 30: 45-50. doi:10.1002/gene.1031. PubMed: 11416862.
38. Inoue K, Kohda T, Lee J, Ogonuki N, Mochida K et al. (2002) Faithful expression of imprinted genes in cloned mice. Science 295: 297. doi: 10.1126/science.295.5553.297. PubMed: 11786635.
39. Ohgane J, Wakayama T, Senda S, Yamazaki Y, Inoue K et al. (2004) The Sall3 locus is an epigenetic hotspot of aberrant DNA methylation associated with placentomegaly of cloned mice. Genes Cells 9: 253-260. doi:10.1111/j.1356-9597.2004.00720.x. PubMed: 15005712.
40. Kang YK, Koo DB, Park JS, Choi YH, Chung AS et al. (2001) Aberrant methylation of donor genome in cloned bovine embryos. Nat Genet 28: 173-177. doi:10.1038/88903. PubMed: 11381267.
41. Dean W, Santos F, Stojkovic M, Zakhartchenko V, Walter J et al. (2001) Conservation of methylation reprogramming in mammalian development: aberrant reprogramming in cloned embryos. Proc Natl Acad Sci U S A 98: 13734-13738. doi:10.1073/pnas.241522698. PubMed: 11717434.
42. Santos F, Zakhartchenko V, Stojkovic M, Peters A, Jenuwein T et al. (2003) Epigenetic marking correlates with developmental potential in cloned bovine preimplantation embryos. Curr Biol 13: 1116-1121. doi: 10.1016/S0960-9822(03)00419-6. PubMed: 12842010.
43. Epsztejn-Litman S, Feldman N, Abu-Remaileh M, Shufaro Y, Gerson A et al. (2008) De novo DNA methylation promoted by G9a prevents reprogramming of embryonically silenced genes. Nat Struct Mol Biol 15: 1176-1183. doi:10.1038/nsmb.1476. PubMed: 18953337.
44. Nowak-Imialek M, Wrenzycki C, Herrmann D, Lucas-Hahn A, Lagutina I et al. (2008) Messenger RNA expression patterns of histone-associated genes in bovine preimplantation embryos derived from different origins. Mol Reprod Dev 75: 731-743. doi:10.1002/mrd.20816. PubMed: 18058811.

RESEARCH ARTICLE

Molecular Reproduction & Development 80:334–348 (2013)

Distribution and Association of mTOR With Its Cofactors, Raptor and Rictor, in Cumulus Cells and Oocytes During Meiotic Maturation in Mice

YUHEI KOGASAKA,* YUMI HOSHINO, YUUKI HIRADATE, KENTARO TANEMURA, AND EIMEI SATO

Laboratory of Animal Reproduction, Graduate School of Agricultural Science, Tohoku University, Sendai, Japan

SUMMARY

Mammalian target of rapamycin (mTOR), a Ser/Thr protein kinase, is the catalytic component of two distinct signaling complexes, mTOR-raptor complex (mTORC1) and mTOR-rictor complex (mTORC2). Recently, studies have demonstrated mitosis-specific roles for mTORC1, but the functions and expression dynamics of mTOR complexes during meiotic maturation remain unclear. In the present study, to evaluate the roles of respective mTOR complexes in maternal meiosis and compare them with those in mitosis, we sought to elucidate the spatiotemporal immunolocalization of mTOR, the kinase-active Ser2448- and Ser2481-phosphorylated mTOR, and raptor and rictor during cumulus-cell mitosis and oocyte meiotic maturation in mice. mTOR principally accumulated around the chromosomes and on the spindle. Phosphorylated mTOR (Ser2448 and Ser2481) exhibited elevated fluorescence intensities in the cytoplasm and punctate localization adjacent to the chromosomes, on the spindle poles, and on the midbody during mitotic and meiotic maturation, suggesting functional homology of mTOR between the two cell division systems, despite their mechanistically distinctive spindles. Raptor colocalized with mTOR during both types of cell division, indicating that mTORC1 is predominantly associated with these events. Mitotic rictor uniformly distributed through the cytoplasm, and meiotic rictor localized around the spindle poles of metaphase-I oocytes, suggesting functional divergence of mTORC2 between mitosis and female meiosis. Based on the general function of mTORC2 in the organization of the actin cytoskeleton, we propose that mTORC1 controls spindle function during mitosis and meiosis, while mTORC2 contributes to actin-dependent asymmetric division during meiotic maturation in mice.

* Corresponding author:
Laboratory of Animal Reproduction
Graduate School of Agricultural Science
Tohoku University
1-1 Tsutsumidori-Amamiyamachi
Aoba-Ku, Sendai 981-8555, Japan.
E-mail: kogayou8539@gmail.com

Grant sponsor: Japan Society for the Promotion of Science; Grant number: 24248047; Grant sponsor: Grant-in-Aid for Young Scientists (B); Grant number: 21780250

Mol. Reprod. Dev. 80: 334–348, 2013. © *2013 Wiley Periodicals, Inc.*

Received 4 December 2012; Accepted 12 February 2013

Published online 26 March 2013 in Wiley Online Library (wileyonlinelibrary.com).
DOI 10.1002/mrd.22166

INTRODUCTION

Immature mammalian oocytes are arrested at the dictyate stage of the first meiotic prophase, also referred to as the germinal vesicle (GV) stage. A pre-ovulatory stimulus induces the resumption of meiosis, morphologically identified by germinal vesicle breakdown (GVBD), and subsequent events, including chromosomal condensation; alignment of the metaphase-I (MI) spindle and its migration to the cortex; segregation of homologous chromosomes;

Abbreviations: AI, anaphase I; GV[BD], germinal vesicle [breakdown]; MI/II, metaphase I/II; MTOCs, microtubule-organizing centers; mTOR[C], mammalian target of rapamycin [complex]; raptor, regulatory-associated protein of mTOR; rictor, rapamycin-insensitive companion of mTOR; TI, telophase I.

emission of the first polar body; and formation of the metaphase-II (MII) spindle. This process is usually defined as meiotic maturation. In addition to the similarity of morphological steps, the machinery governing female meiotic progression often shares common features with the analogous mitotic process of somatic cells (Solc et al., 2010). In contrast, in the meiotic spindle, alternative mechanisms of spindle assembly and relocation are predominant because oocytes are often devoid of canonical centrosomes and astral microtubules (Szollosi et al., 1972). In mammalian oocytes, microtubule-organizing centers (MTOCs) form the spindle in place of centrosomes (Schatten and Sun, 2009), and the meiotic spindle migrates to the cortex in an actin-dependent manner, rather than requiring astral microtubules (Longo and Chen, 1985; Verlhac et al., 2000; Gonczy, 2008).

The mammalian target of rapamycin (mTOR), an evolutionarily conserved and ubiquitously expressed Ser/Thr protein kinase, forms the catalytic core of at least two functionally distinct complexes, mTOR complex 1 (mTORC1) and mTOR complex 2 (mTORC2). Each complex shares mTOR, mLST8/GβL, and deptor; mTORC1 contains raptor and PRAS40 while mTORC2 contains rictor, mSin1, and PRR5/protor (Bhaskar and Hay, 2007; Jacinto and Lorberg, 2008; Alessi et al., 2009; Cybulski and Hall, 2009; Dunlop and Tee, 2009; Laplante and Sabatini, 2009; Foster and Fingar, 2010). The molecular function of these cofactors remains poorly understood, although the scaffold proteins raptor and rictor have been shown to be required for the downstream effects of their respective complexes, permitting mTOR to bind directly to definite substrates (Kim et al., 2002; Kim and Sabatini, 2004; Wullschleger et al., 2005). Generally, mTORC1 is known to control protein synthesis, cell growth, cell proliferation, and cell cycle progression (Fingar et al., 2002, 2004; Schalm et al., 2003; Fingar and Blenis, 2004; Ruvinsky and Meyuhas, 2006), whereas mTORC2 is associated with control of the organization of the actin cytoskeleton (Jacinto et al., 2004; Sarbassov et al., 2004). In mitotic cells, Ser2448- or Ser2481-phosphorylated mTOR, biomarkers of intrinsic mTOR catalytic activity (Altomare et al., 2004; Lawrence et al., 2004; Yonezawa et al., 2004), and raptor have been shown to exhibit strong expression and have been linked to the localization of the mitotic apparatus (Yaba et al., 2008; Vazquez-Martin et al., 2009a, 2012; Doghman et al., 2010; Lopez-Bonet et al., 2010; Yu et al., 2011). Furthermore, functional studies have demonstrated that mTORC1 is involved in regulation of centrosome number, spindle shape, and chromosome segregation (Bonatti et al., 1998, 2005; Yonezawa et al., 2004; Astrinidis et al., 2006, 2010; Gui et al., 2007; Yu et al., 2011, 2012). Thus, mTORC1 is implicated in mitotic spindle function during the mitotic phase.

Recently, mouse oocyte studies have shown that mTOR mRNA is expressed during oocyte maturation and that mTOR localizes in the nucleus at the GV stage, around the chromosomes at GVBD, and on the spindle at the MII stage. Functional analysis using inhibitor treatment and injection of mTOR antibodies has also revealed that mTOR is involved in GVBD, spindle relocation, and first polar body emission (Yan-Chang and Cai-Rong, 2009; Lee et al., 2012). These reports suggest that, in addition to its roles during mitosis, mTOR participates in many steps of oocyte meiotic maturation, although its detailed roles, particularly focusing on functional variations of each complex, are still unclear. In the present study, we investigated the distribution of mTOR, Ser2448- and Ser2481-phosphorylated mTOR, and components of mTORC1 and mTORC2 during mitosis of cumulus cells versus oocyte maturation in mice in order to compare the distributions and functions of these proteins in mitosis and oocyte meiosis. Here, we report that mTOR and raptor colocalized on the spindle, and phosphorylated mTOR was strongly expressed at spindle poles as well as the midbody in both cumulus cells and oocytes. Rictor was markedly localized around spindle poles only in MI oocytes. These data indicate that mTORC1 may be associated with spindle functions in both mitosis and oocyte maturation, while mTORC2 may control meiotic spindle migration.

RESULTS

Distribution of mTOR and Phosphorylated mTOR in Mouse Cumulus Cells

To examine the distribution of mTOR in mouse cumulus cells, we first performed immunofluorescence staining with antibodies against mTOR and kinase-active Ser2448- and Ser2481-phosphorylated mTOR (pS2448-mTOR and pS2481-mTOR, respectively). In vivo ovulatory stimuli in mice have been reported to induce temporal upregulation of the proliferative capacity of cumulus cells, corresponding to early oocyte meiotic maturation (Hernandez-Gonzalez et al., 2006). Thus, we collected cumulus oocyte complexes 8 hr after culture, the period at which almost all oocytes have progressed to the first meiotic division, in order to obtain cumulus cells in various stages of the cell cycle. Throughout the layer of cumulus cells, mTOR, pS2448-mTOR, and pS2481-mTOR were localized throughout the entire cell (Fig. 1A–I). Notably, when classifying cumulus cells by their nuclear status (Fig. 1A, D, and G), mitotic cumulus cells were also observed in this in vitro maturation system, we observed higher expression levels of pS2448-mTOR and S2481-mTOR in mitotic-phase cells than in other phases of the cell cycle (Fig. 1E–F and H–I).

Intracellular Localization Dynamics of mTOR and Phosphorylated mTOR During Mitotic Progression in Mouse Cumulus Cells

To elucidate the precise distribution of mTOR during mitosis, we followed the intracellular immunolocalization of mTOR, pS2448-mTOR, and pS2481-mTOR during the progression of mitosis in cumulus cells. mTOR, pS2448-mTOR, and pS2481-mTOR were expressed in the cytoplasm at all stages, but the localization of intense expression changed during mitotic progression

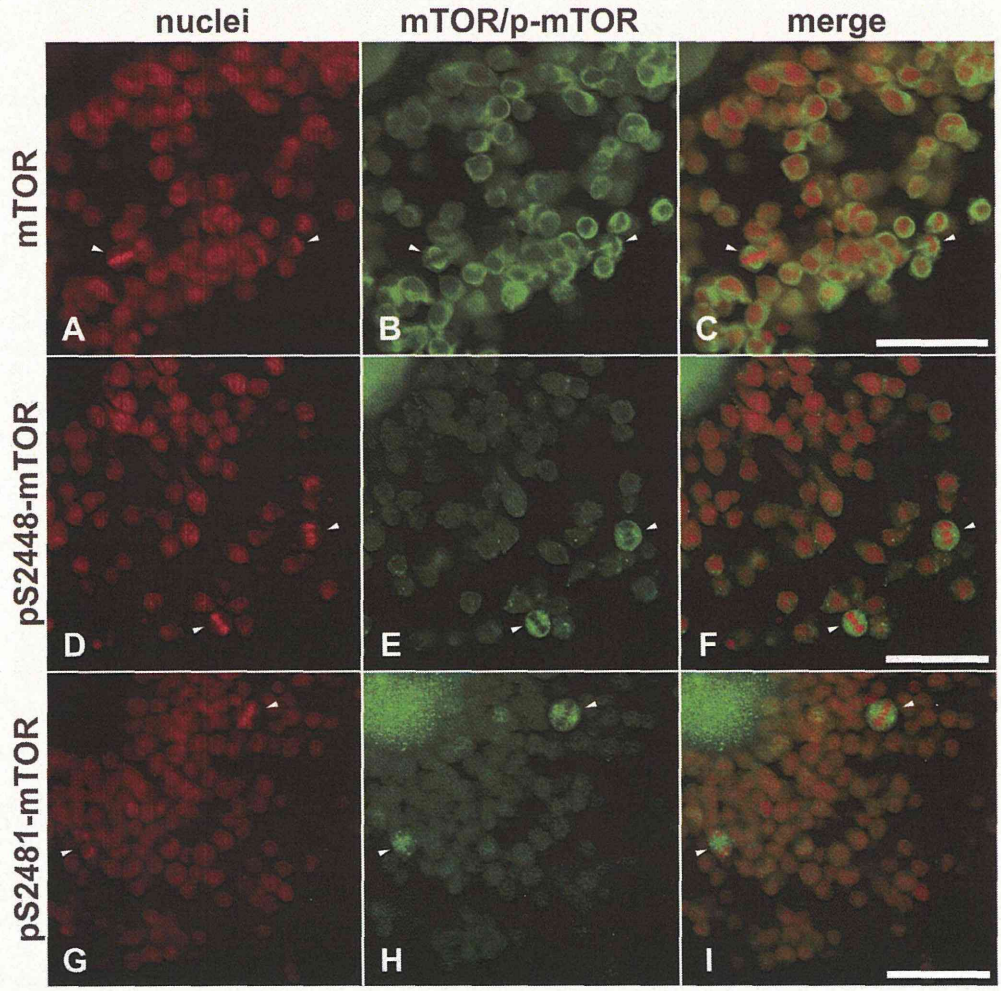

Figure 1. Immunolocalization of mTOR and phosphorylated mTOR in mouse cumulus cells. The panels show nuclei (**A**, **D**, **G**), mTOR or phosphorylated mTOR (p-mTOR; **B**, **E**, **H**), and merged images (**C**, **F**, **I**). Red and green represent nuclei and mTOR/p-mTOR, respectively. The arrowhead indicates mitotic cells. Scale bar, 50 μm.

(Fig. 2Aa–Cf). At interphase, mTOR was distributed mainly in the cytoplasm and subtly in the nucleus (Fig. 2Aa), but was localized principally around the chromosomes at prophase (Fig. 2Ab) and on the spindle between metaphase and cytokinesis (Fig. 2Ac–Af). Both pS2448-mTOR and pS2481-mTOR were distributed in the cytoplasm and in the nucleus at interphase (Fig. 2Ba and Ca), despite the intense speckled pattern localization that was observed adjacent to the chromosomes at prophase (Fig. 2Bb and Cb), on the spindle poles between metaphase and telophase (Fig. 2Bc–Be and Cc–Ce), and on the spindle poles as well as on the midbodies at cytokinesis (Fig. 2Bf and Cf). We observed speckled patterns in the periphery of the cytoplasm for pS2448-mTOR, as shown in the image of telophase (Fig. 2Be). A speckled pattern was observed in the cytoplasm for pS2481-mTOR, including the spindle area (Fig. 2Da–Fd).

Distribution of mTOR, Raptor, and Rictor in Mouse Cumulus Cells

To assess the distribution and colocalization of raptor and rictor with mTOR in mouse cumulus cells, we executed triple staining with antibodies against mTOR, raptor, and rictor. We first confirmed that the same distributions were obtained with triple staining and single staining methods for raptor and rictor (data not shown). Raptor expression and colocalization with mTOR was observed throughout the entire layer of cumulus cells (Fig. 3C and E). Although rictor was also expressed throughout the cumulus cell layer, we